Partially Constrained Recovery of (Meth)acrylate Shape-Memory Polymer Networks

Nishant Lakhera,[1] Christopher M. Yakacki,[2] Thao. D. Nguyen,[3] Carl P. Frick[1]

[1]Department of Mechanical Engineering, University of Wyoming, Laramie, Wyoming 82071
[2]Department of Mechanical Engineering, University of Colorado Denver, Denver, Colorado 80217
[3]Department of Mechanical Engineering, Johns Hopkins University, Baltimore, Maryland 21218

ABSTRACT: The purpose of this study was to characterize the partial strain recovery of a thermoset shape-memory polymer under a constraining stress. Three polymer networks were synthesized from *tert*-butyl acrylate and poly(ethylene glycol) dimethacrylate (PEGDMA) solutions. The molecular weight and the weight fraction of the PEGDMA crosslinking monomer was altered systematically to maintain a constant glass transition temperature ($T_g = 54°C$) but tailorable rubbery moduli, which varied by almost an order of magnitude for the three polymer networks ($E'_r = 1.8–11.3°MPa$). The shape-recovery behavior of the polymers under a constraining stress was characterized for programming temperature below (20°C) and above (70°C) the T_g. The experiments revealed a peak in the recovered strain for samples programmed at 20°C. Recovered strain scaled linearly with the constraining stress by the rubbery modulus. The work performed by the shape-memory polymer networks was observed to be primarily a function of constraining stress and crosslinking density, while programming temperature had a relatively mild influence; however, the efficiency of the shape-memory effect was shown to be a function of constraining stress and programming temperature, but was independent of crosslinking density. Maximum work efficiencies (up to 45%) were observed for programming temperature of 70°C. © 2012 Wiley Periodicals, Inc. J Appl Polym Sci 000: 000–000, 2012

Key words: stimuli-sensitive polymers; structure-property relations; compression; glass transition; thermosets

INTRODUCTION

The shape-memory effect in polymers refers to a polymer's ability to recover to a predefined shape in response to a stimulus, most often triggered by an increase in the thermal energy.[1] The shape-memory cycle consists of deforming the polymer at a programming temperature, then decreasing the temperature below a critical temperature (e.g., glass transition temperature, T_g) such that the deformation is stored. Upon heating, the polymer transitions into a new state, and applied storage strain is recovered. When compared with the traditional shape-memory alloys such as nickel-titanium that can recover $\sim$ 4–12%[2,3] of the applied deformation, shape-memory polymers (SMPs) can recover strain on the order of 50–800%.[4,5] Other inherent advantages of the SMPs include low-density, low-manufacturing costs, ease of processing,[6,7] wide range of transition temperatures, biodegradability,[8] and biocompatibility.[9] SMPs have been proposed for a variety of applications, including self-deployable structures for biomedical[10]

and space applications,[11,12] and degradable SMPs have been used in construction of vascular related products.[8,13,14] SMP based micro-actuators have been integrated into the soft lithography fabrication technology with minimal processing.[15–17]

The majority of research studies have investigated the recovery behavior of SMPs under two test conditions: unconstrained recovery in the absence of an applied stress or fully constrained recovery to measure the stress generation. These conditions represent the extremes in SMP behavior, demonstrating either the maximum potential recoverable strain or the maximum actuation stress. With respect to shape recovery in SMPs, several variations of unconstrained and fully constrained recovery conditions have been studied, as shape-memory recovery is a temperature/time dependent process. Studies which have focused on understanding the fundamental mechanisms that control shape-memory behavior utilize slow heating in an attempt to limit inhomogeneous temperature distribution throughout the sample.[18] For instance, Castro et al. utilized specially manufactured compression platens to aid in heat transfer during stress–strain testing during strain recovery.[18] Research based on developing new applications and increasing the functionality of the SMPs have concentrated on heating conditions likely to be experienced during

usage.[19,20] Studies have also showed that when SMP with fixed deformation was heated for recovery, an actuation stress is generated against the platens when the temperature approaches and exceeds T_g.[21–23]

Neither unconstrained nor fully constrained conditions are likely to be realized for the majority of SMP applications. It is far more probable that in actual service, the SMP will be partially constrained, meaning that the material will be allowed to recover under an applied stress below the maximum stress required for programming shape-memory. For example, SMPs have been investigated for use as self-deployable cardiovascular stents.[24–26] Stents are expandable scaffolds designed to support blood vessels and have been shown to have a clinical benefit after balloon angioplasty. For this application the SMP stent would be deformed to a minimal profile, positioned in the vessel, and allowed to expand against the vessel walls. It is critical that the SMP not deploy completely against the vessel wall because the frictional force must be large enough to keep the stent in place, as well as prevent vasospasms and restenosis; however, the SMP stent must deploy sufficiently to allow for improved blood flow. In this example, the SMP partially recovered the maximum possible strain, and partially realized the maximum possible actuation stress. To the authors' knowledge, no previous researchers have systematically characterized the intermediate behavior between these two maximums.

In addition to explicitly demonstrating partially constrained recovery behavior, this study also investigates the potential recoverable work in SMPs. Although, SMPs are often suggested for use as actuators,[27–30] very few studies have investigated the work density of SMPs. Rapp et al. introduced an experimental procedure to determine the recovery work density using closed-loop force controlled thermo-mechanical cycling.[30] This study discovered that for moderate maximum strains, the performance of SMP actuators in compression is better than in tension because of the superposition of the thermal expansion and the shape-memory effect. It was also shown that low-mass of the SMPs leads to high-specific energy densities, which is advantageous for application in lightweight structures. Kolesov et al. measured the mechanical work generated by release of the stored energy and resulting stress during shape recovery under 0.1 or 0.2 MPa applied load.[31] The work generated by the programmed specimen during thermally induced recovery was shown to moderately increase with crosslinking density, despite the substantial increase in programming stress. Kolesov et al. explicitly suggested that SMP work could be used as a design criterion of practical relevance.[31] Unfortunately, the study did not consider the effect of the programming temperature

being above or below the T_g. Pandini et al. showed that a certain amount of energy is stored within the material as a consequence of the specimen's cooling during the shape-memory programming stage, which is later released over a large temperature range during recovery stage.[32] This study also proposed that the ratio of stored energy to the energy required for deformation is about 0.5 for temperatures up to T_g. Unfortunately, none of these studies have systematically investigated recovery from a practical perspective utilizing partially constrained recovery.

The presented research fills the gaps in the current research landscape by investigating partially constrained shape recovery of SMPs, and quantifies the performance by calculating the recoverable work and efficiency of the recovery process. Therefore, three previously investigated photopolymerizable (meth)acrylate SMP networks were chosen.[26] Compressive samples were machined from each of these SMPs and deformed at temperatures both above and below T_g, in order to capture the effect of programming temperature on recovery behavior. Results demonstrate that samples programmed below T_g initiate shape-memory strain recovery at lower temperatures, and under relatively large constraining stresses can exhibit a recovery maximum near T_g before reaching equilibrium conditions at higher temperatures. The work performed per unit volume by the three SMP networks was quantified as a function of constraining stress. Results obtained show that the maximum work output scaled with the magnitude of the rubbery modulus; however, the efficiency was similar for all materials for the same programming temperature. It was also observed that to obtain highest efficiency from the SMP, samples should be allowed to recover approximately half the initial deformation under constraining stress.
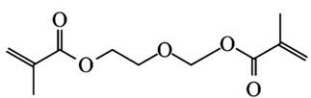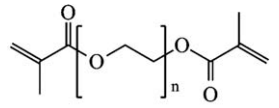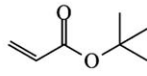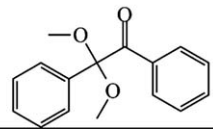
EXPERIMENTAL

Materials

Poly(ethylene glycol) dimethacrylate (PEGDMA) with an average molecular weight of $M_n = 550$, Di(ethylene glycol)dimethacrylate (DEGDMA) with an average molecular weight of $M_n = 242$, tert-butyl acrylate (tBA), and the photoinitiator 2,2-Dimethoxy-2-phenyl-acetophenone (DMPA) were procured from Sigma Aldrich and used in their as received conditions without any further purification. The names, abbreviations, chemical structures, and molecular weights of all the constituents can be found in Chart 1.

Polymer synthesis

A crosslinker solution (XLS) was created by mixing 30 wt % DEGDMA with 70 wt % PEGDMA. The

Chart 1 Names, abbreviations, structures and molecular weights of the base constituents used.

XLS solution was chosen to maintain a constant T_g when copolymerized with tBA, regardless of the amount of XLS. The tBA-co-XLS networks were then synthesized by free-radical polymerization using 0.1 wt % DMPA photoinitiator. All solutions were mixed thoroughly by hand for 30 s followed by 5 min in an ultrasonic shaker (Branson 2510) to ensure a well-distributed solution. The polymer solution was injected either between two glass slides separated by glass spacers, or into a cylindrical polyethylene mold, depending on subsequent testing to be performed. For the glass slides, polymerization was performed in a UV crosslinker oven (UVP, CL1000) for 15 min. For the cylindrical molds, specimens were polymerized under a UV lamp (Blak Ray B100 A/R) for 15 min. Following UV curing, all polymer samples were placed in an oven at 90°C for 1 h to ensure complete polymerization.

Characterization by DMA

Dynamic mechanical analysis (DMA) was used to characterize the low-strain thermo-mechanical properties of the networks using a TA Instruments Q800 DMA. The samples cured from the glass slides were cut into small rectangles and lightly sanded with coarse grit sandpaper to remove surface imperfections. These samples were tested under tensile loading with the sample dimensions measuring $\sim$ 25.0 $\times$ 5.0 $\times$ 1.0 mm^3. The samples were thermally equilibrated at -50°C for 5 min and heated to 150°C at a rate of 5°C/min while subjected to a 0.1% dynamic strain at 1 Hz. T_g was defined as the peak of the

tan δ curve. Duplicate tests were run to ensure repeatability. The onset of glass transition, T_{onset}, was calculated using an intersecting line method at the initial drop in glassy modulus, where the starting point of the left tangent line was T_g -50°C and the starting point of the right tangent line was the T_g. The rubbery modulus, E_r' was defined as the lowest point in the rubbery plateau.

Partially constrained recovery

Load-controlled strain recovery tests were conducted on a MTS hydraulic load frame (MTS 858 Mini Bionix II) equipped with a MTS 651 environmental chamber, a liquid nitrogen cooling mechanism and a laser extensometer (MTS LX 500). These experiments involved a three-step process that included initial isothermal deformation, followed by temperature induced shape storage, and subsequent thermally induced strain recovery under an applied stress. The cylindrical samples of each network were machined to $\sim$ 10 mm in diameter, with a length to diameter ratio of 1.5 : 1. During deformation, samples were thermally equilibrated in the temperature-controlled chamber to 20 or 70°C for 30 min. The samples were compressed to 30% strain at a displacement rate of 0.01 mm/s and held for 20 min to allow for stress relaxation. Next, the samples were cooled to 0°C at a rate of 5°C/min and annealed at the lower temperature for 10 min. The stress decreased to zero during the cooling and annealing period, indicating the sample contraction away from the platens. A constraining stress, σ_A, was then applied to the samples. The samples were heated up to 100°C at a rate of 2°C/min and strain recovered under the constraining stress was measured as a function of temperature.

RESULTS AND DISCUSSION

Thermo-mechanical characterization of polymer networks

As the purpose of this study was to characterize partially constrained recovery of SMPs, it was appropriate to select a material that has already been well studied. Meth(acrylate)-based SMPs were chosen based on previous work by the authors.[9,21,23,26,33–37] The primary advantage of these materials is the ability to tailor the thermo-mechanical properties, as T_g and E_r' can be optimized independently from one another.[26,36] As a result, three polymer networks were created with near equal T_g, but varied nearly an order of magnitude in terms of the E_r'.[26] These three shape-memory polymer networks have already been investigated and demonstrated good biocompatibility for potential use in biomedical devices.[26]
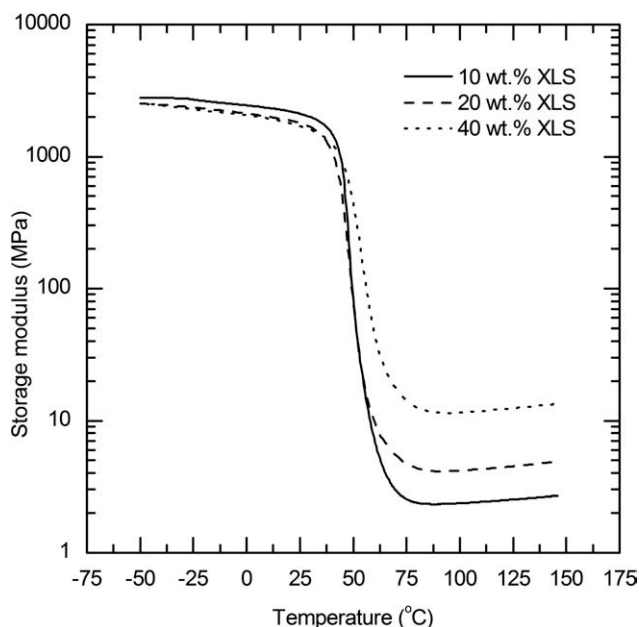
Figure 1 Dynamic mechanical analysis measurements of copolymers comprised of *tert*-butyl acrylate monomer polymerized with poly(ethylene glycol) dimethacrylate crosslinker. Polymer networks were tailored to vary in rubbery modulus, E_r' with a constant glass transition temperature, T_g. The sample with 10 wt % XLS, 20 wt % XLS, and 40 wt % XLS are represented by solid, dashed, and dotted line, respectively.

Representative DMA curves of the three networks are shown in Figure 1. The curves are singular representations chosen from 3 to 5 repeatable tests. Each polymer network was created by photopolymerizing *t*BA with a PEGDMA-based XLS, as described in the Experimental Section. The weight fractions and molecular weights of the constituents were carefully manipulated such that all three materials exhibited the same T_g but significantly different E_r'. As observed from Figure 1, the T_g for the three networks was almost the same with average values of 53.3, 53.4, and 57.1°C for 10, 20, and 40 wt % XLS samples, respectively. The networks clearly exhibited a well-defined transition from the glassy state to the rubbery state, which is the characteristic of a thermoset SMP.[7] The rubbery modulus of the networks varied directly with higher density of chemical crosslinks across the covalently bonded monomer chains. The inherent advantage of systematically varying E_r' is that it allows for tailoring the stiffness to better match with potential application. It should be noted that the addition of crosslinker beyond 40 wt % would widen the transition regime, preventing the transition from glassy to rubbery region from being well defined. The crosslinking density of the three networks was also quantified. For an elastomeric network the crosslinking density, v, has

been shown to be related to rubbery modulus through the equation[34]

$$E_r' = 3vRT \qquad (1)$$

where R is gas constant, E_r' is the rubbery modulus, and T is the absolute temperature at which E_r' is measured. Therefore, crosslinking density is directly proportional to the rubbery modulus. The crosslinking densities of the three networks were calculated using eq. (1) using an absolute temperature of 70°C (343.15 K) and its corresponding E_r'. The results shown in Figure 1 clearly demonstrate that increasing wt % XLS in the polymer networks resulted in an increase in the crosslinking density of the network, which is reflected by the higher E_r' values. A summary of thermo-mechanical properties as obtained from DMA analysis and the crosslinking density, v, of the three networks is presented in Table I. It should be noted that the values presented are average values obtained from 3 to 5 tests. Table I also represents one standard deviation obtained from 3 to 5 repeatable tests.

Partially constrained recovery characterization

Compressive testing was performed to investigate the partially constrained recovery behavior of the polymer networks. Testing was performed at two deformation temperatures, 20 and 70°C, to represent temperatures well below and well above T_g, respectively. Figure 2 shows representative compressive stress–strain response of the three networks equilibrated at 70°C. At this elevated temperature, classic elastomeric behavior was demonstrated by all of the networks. Figure 2(a) shows singular representative stress–strain curves from 3 to 5 repeatable tests. The elastic slope of the elastic stress–strain curve was proportional to the crosslinking density, and matched fairly well with the DMA results (Fig. 1). The 40 wt % XLS samples exhibited the highest slope and stress values, while the 10 wt % XLS samples exhibited the lowest. The reason for this was the higher rubbery modulus of the 40 wt % XLS samples at 70°C, which is correlated to the higher crosslinking density of the 40 wt % XLS samples. Samples deformed to 30% strain were held isothermally for 20 min, the representative curves for which are shown in Figure 2(b). The samples being in the rubbery regime did not demonstrate any appreciable time-dependent stress relaxation. The material at higher temperature behaved like a purely elastic material and therefore the stress remained relatively constant with time, as indicated by a straight line in Figure 2(b). Removing the applied stress allowed the material to recover all the deformation (results not shown).

TABLE I
Thermo-Mechanical Properties of the Polymer Networks as Obtained from DMA Analysis

XLS (wt %)	tBA (wt %)	T_{onset} (°C)	T_g (°C)	E_r' (MPa)	ν (mol/m^3)
10	89.9	45.16 ± 0.27	53.31 ± 0.03	1.82 ± 0.03	309
20	79.9	43.72 ± 1.48	53.35 ± 0.76	3.97 ± 0.41	635
40	59.9	45.23 ± 0.37	57.11 ± 0.61	11.23 ± 0.33	2022

The numbers represents the average values and one standard deviation obtained from 3 to 5 repeatable tests. The networks exhibited almost same T_g but varied significantly in their E_r'. Also included are the crosslinking densities obtained for the polymer networks.

Figure 3(a) shows representative stress–strain curves for three networks deformed at 20°C. The initial loading was elastic, showing a linear stress–strain relationship followed by yielding at stresses ranging from 55 to 63 MPa. Soon after the yield point was surpassed, the stress dropped significantly to values between 40 and 45 MPa. This softening is typical for plastic deformation of thermoset polymers caused by local segmental rotation. With increasing strain local polymer chains became aligned, and the sample started to harden, as represented by the mild increase in stress with the corresponding increase in strain in Figure 3(a). It can be seen from Figure 3 that at 20°C the modulus, yield stress, and general shape of all three networks were very similar. The displacement ramp was stopped once 30% deformation was achieved and samples were held for 20 min to measure the stress relaxation response. The materials being in the glassy regime demonstrated significant stress relaxation. The magnitude of the stress relaxation scaled with the crosslinking density. Figure 3(b) showed that 10 wt % XLS samples relaxed to the lowest stress level, while 40 wt % XLS samples relaxed to the highest stress level because it exhibited the higher E_r'.

Following compression and relaxation, all samples were held in place and cooled to 0°C at a rate of 5°C/min to fix the deformed shape. As the temperature decreased, the stress value dropped to zero, as thermal contraction eventually separated the programmed samples from the compression platens. The samples were then held at 0°C for 10 min to ensure thermal equilibrium. A constraining stress, σ_A was then applied on the samples, which were subsequently heated to 100°C at a rate of 2°C/min to allow strain recovery under an applied stress. The constraining stress values were selected such that the same stress could be applied to samples programmed at 70 and 20°C.

Representative partially constrained recovery curves can be seen in Figures 4 and 5. Specifically, they represent the normalized recovered strain as a function of temperature for 20 wt % XLS samples, programmed to 30% strain at 70°C (Fig. 4) and 20°C (Fig. 5), respectively. For programming above T_g (70°C), strain recovery was not activated until the sample temperature reached T_{onset}, which was followed by rapid strain recovery over a narrow temperature range (~ 45–60°C). The maximum recoverable strains of the samples experienced a plateau with increasing temperature in the rubbery regime, while the amount of strain recovery was inversely proportional to σ_A.

The characteristics of strain recovery displayed several notable differences for programming below T_g (20°C). In this case, strain recovery was initiated around the programming temperature, 20°C, which is well below T_{onset}. Previous studies have shown that the programming temperature is correlated to the initiation of shape recovery.[23,38] Programming below T_g is believed to store more internal (mechanical) energy in addition to entropic energy, which initiated the shape-memory effect at lower temperature levels. Closely observing Figure 5, for low-levels of σ_A, samples experienced a plateau in recovery strain similar to the samples programmed above T_g; however, samples which were constrained by higher amounts of stress showed a peak in the recovered strain, followed by a reduction in recovered strain with increasing temperature. The reduction from the peak strain value eventually reached the same plateau as the samples programmed above T_g. It should be noted that the peak recovered strain values of these samples were significantly higher than their counterparts. For example, at 1.3 MPa of constraint, samples programmed above T_g showed no appreciable recovery at 50°C and 10% strain recovery at 70°C, whereas the samples programmed below T_g showed 30% strain recovery at 50°C and 10% strain recovery at 70°C. In previous studies a peak in stress generation was seen in samples under full constraint.[21,22] The stress peak phenomenon was primarily associated with thermal expansion in the glassy state, but other factors such as heating and cooling rates were also shown to influence its magnitude.[39] The current results showed a previously unreported strain recovery peak under stress constraint that appears analogs to the stress generation peak under full constraint condition. However, the thermal expansion alone cannot account for the magnitude of this peak, which is
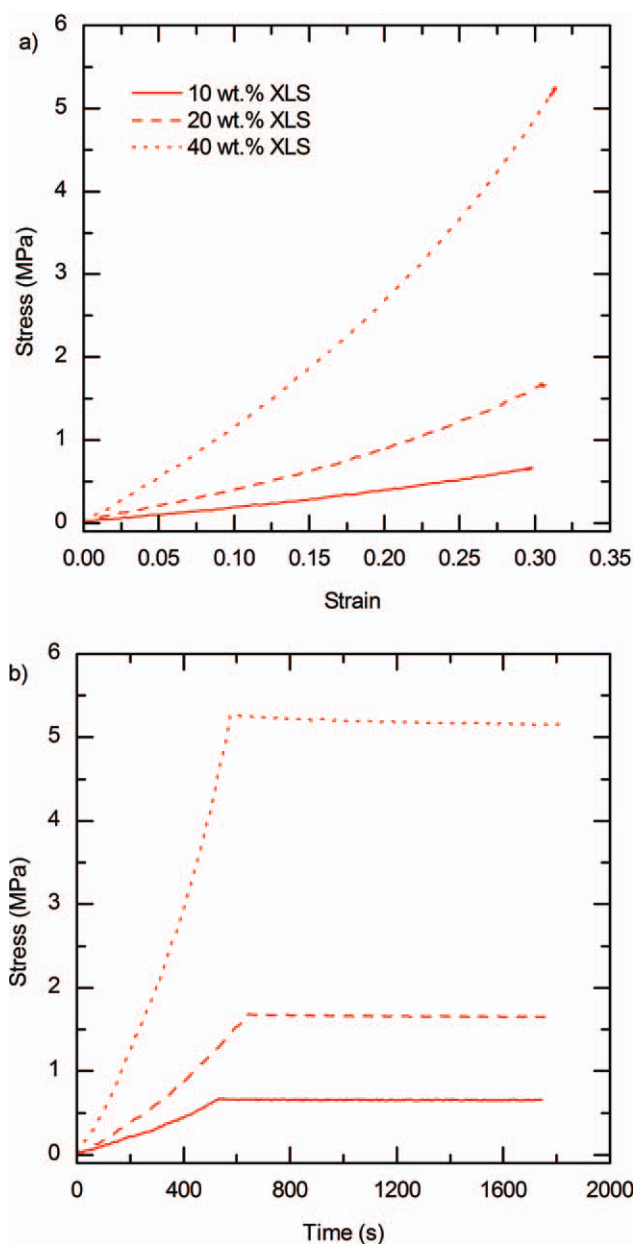
Figure 2 (a) Elastic stress–strain response for 10 wt % (solid line), 20 wt % (dashed line), and 40 wt % XLS samples (dotted line), and (b) stress-time response for the same networks programmed at 70°C. The 40 wt % XLS samples required more stress to be deformed by same amount owing to its high rubbery modulus. The slope of the stress–strain curve also scaled with the crosslinking density. No stress relaxation is observed for all three crosslinking densities. [Color figure can be viewed in the online issue, which is available at wileyonlinelibrary.com].

on the order of 20% normalized recovered strain. It is clear that the samples are recovering deformation at lower temperatures as the material undergoes the glassy-to-rubbery transition, and thereby maximum recovery strains are realized at temperatures near T_g. These results suggested that samples programmed below T_g have a higher work capacity under increased amounts of constraint. A detailed paramet-

ric study by the authors is underway to investigate the underlying mechanisms of this strain recovery peak based on a thermo-viscoelastic model for amorphous SMP.[22] The normalized recovered strain as a function of temperature gave analogs results for 10 and 40 wt % XLS samples for both programming temperatures.
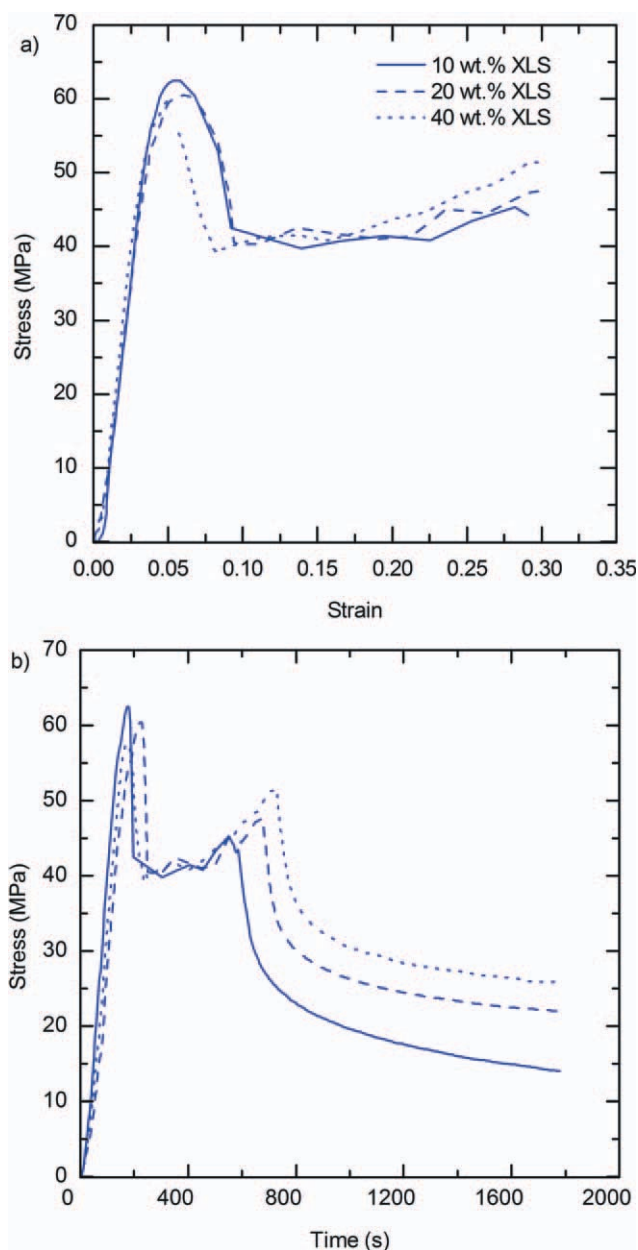
Figure 3 (a) Stress–strain response for 10 wt % (solid line), 20 wt % (dashed line), and 40 wt % XLS samples (dotted line), and (b) stress-time response for the same networks programmed at 20°C. Significant stress relaxation is observed for all three crosslinking densities due to the materials being the glassy regime. The 10 wt % XLS samples relaxed to the lowest stress levels and 40 wt % XLS to the highest stress level. [Color figure can be viewed in the online issue, which is available at wileyonlinelibrary.com].
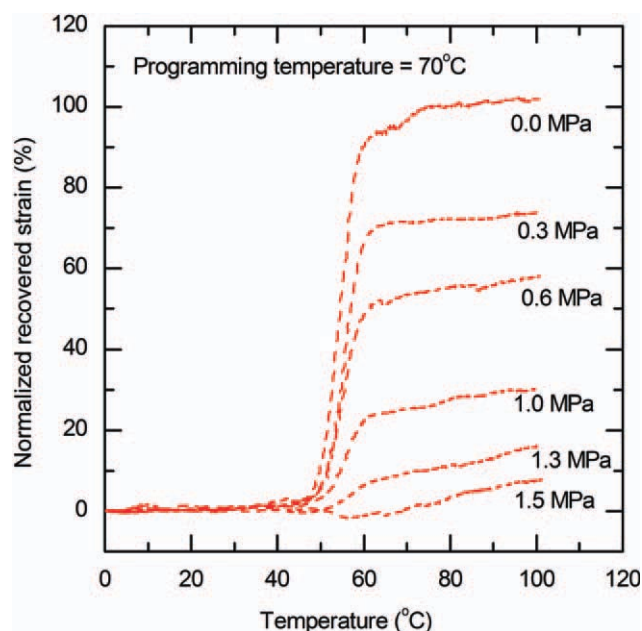
Figure 4 Normalized recovered strain as a function of temperature for 20 wt % XLS samples, programmed at 70°C. A constraining stress was applied on the samples and were subsequently heated for recovery to characterize the partially constrained strain recovery behavior. The strain recovered decreased with the increase in the applied constraining stress. The 10 and 40 wt % XLS samples demonstrated analogs results. [Color figure can be viewed in the online issue, which is available at wileyonlinelibrary.com].
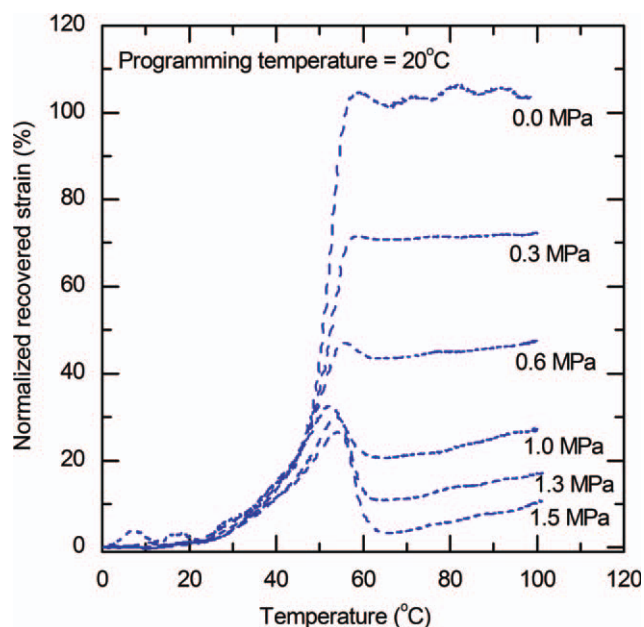
The partially constrained recovery behavior as a function of σ_A for all three crosslinking densities is quantified in Figure 6. Two recovered strains were defined: (a) normalized recovered strain at 70°C, ε_R, and (b) maximum normalized recovered strain at or below 70°C, ε_{RMA}. Figure 6(a) shows the behavior of samples programmed at 70°C, for all crosslinking densities. As expected, σ_A values are higher for specimens with higher crosslinking densities. For the samples programmed at 70°C no strain recovery peak was observed, therefore, $\varepsilon_R = \varepsilon_{RMA}$ (Fig. 4). The ε_R value for $\sigma_A = 0$ MPa was expected to be 100%, neglecting the effect of thermal expansion. The relationship between ε_R and σ_A was observed to be near linear for samples programmed at 70°C. Figure 6(b) represents a similar curve for samples programmed at 20°C. For these samples, $\varepsilon_R \neq \varepsilon_{RMA}$, because of the strain recovery peak observed for samples under high σ_A (Fig. 5). Results showed that ε_R scaled linearly with σ_A, and that σ_A values were higher for samples with higher crosslinking densities, similar to Figure 6(a). These results are in a relatively good agreement to the hypothesis proposed by SMP researchers that a linear relationship exists between the actuation stress and the recoverable strain for samples tested above and below the T_g.[38] The value of ε_R for a given σ_A correlated with

the E_r' (from DMA analysis), for any given temperature, which substantiates that the shape recovery is driven by the entropic rearrangements of the amorphous network above the T_g to its equilibrium configuration. Figure 6(b) also represents the ε_{RMA} as a function of σ_A, for samples of all crosslinking densities programmed at 20°C (shown with open circles). For a relatively low σ_A, the linear relationship between the σ_A and the ε_{RMA} held true. This is because the recovered strain was near maximum at 70°C for relatively low applied loads. However, with increasing σ_A, a local maximum in ε_{RMA} occurred at approximately T_g (Fig. 5). Because of this strain recovery peak, the linear relationship became truncated with increasing σ_A [Fig. 6(b)]. For the same high σ_A values, ε_{RMA} was higher than ε_R, independent of the crosslinking density.

Work and efficiency of SMPs

To better characterize the partially constrained recovery behavior, the work performed by the SMP under a constraining stress during heating was calculated. Two SMP works were defined: (a) SMP work performed at 70°C:

$$W_R = \sigma_A \varepsilon_R \qquad (2)$$

Figure 5 Normalized recovered strain as a function of temperature for 20 wt % XLS samples, programmed at 20°C. A constraining stress was applied on the samples and were subsequently heated for recovery, to characterize the partially constrained strain recovery behavior. Samples constrained by higher stresses showed a peak in the recovered strain, close to the T_g, followed by a reduction in recovered strain with increasing temperature. [Color figure can be viewed in the online issue, which is available at wileyonlinelibrary.com].
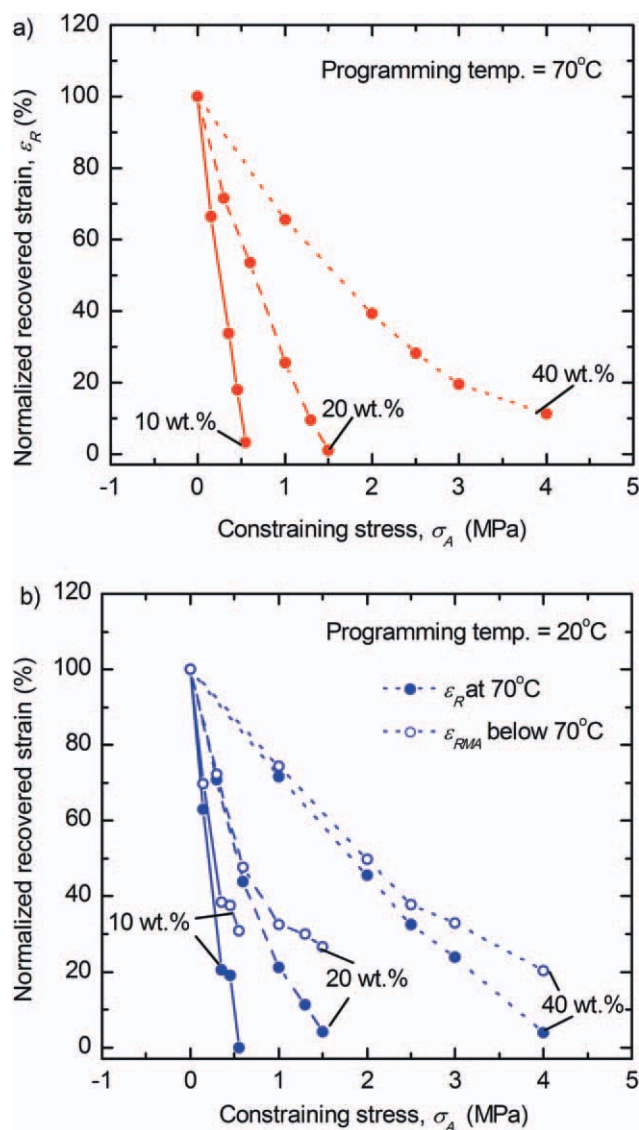
Figure 6 Normalized recovered strain as a function of constraining stress for all samples tested. (a) Recovered strain at 70°C as a function of constraining stress for the samples programmed at 70°C. A linear relationship was observed between recovered strain at 70°C and constraining stress for all crosslinking densities, and (b) recovered strain as a function of constraining stress for samples programmed at 20°C. For this the recovered strain at 70°C (closed circles), also followed a linear relationship with the constraining stress, while the maximum recovered strain at or below 70°C (open circles), had a near linear relationship for low-constraining stresses, but it truncated out for higher constraining stresses due to the strain recovery peak (Fig. 5). [Color figure can be viewed in the online issue, which is available at wileyonlinelibrary.com].

where, σ_A is the constant applied constraining stress during recovery heating, and ε_R is the recovered strain at 70°C, and (b) Maximum SMP work performed at or below 70°C:

$$W_{\mathrm{RMA}} = \sigma_A \varepsilon_{\mathrm{RMA}} \qquad (3)$$

where, $\varepsilon_{\mathrm{RMA}}$ is the maximum recovered strain at or below 70°C. Strictly speaking, the work calculated in eqs. (2) and (3), was the work performed per unit volume of the SMP (kJ/m^3).

Using the values shown in Figure 6 and eqs. (2) and (3), both W_R and W_{RMA} for the SMP were calculated and plotted as a function of σ_A, as shown in Figure 7. Figure 7(a) shows W_R as a function of σ_A, for samples programmed at 70°C. W_R was defined as zero at the two ends of the curve, as either no actuation stress or strain recovery was possible for either unconstrained ($\sigma_A = 0$ MPa) or fully constrained ($\varepsilon_R = 0\%$) testing, respectively. For the same crosslinking density, W_R first increased from zero for unconstrained condition, reached a maximum, and then decreased with further increase in σ_A until it finally reached zero again for fully constrained condition. The maximum was observed close to $\sim 50\%$ strain recovery. This result has important implications for engineering design using SMPs. Between the two extremes, W_R was therefore seen to be a symmetric and half-elliptical shape. As E_r' increased with the increase in crosslinking density, the magnitude of W_R also increased with the crosslinking density, independent of the programming temperature. The effect of crosslinking density was earlier stated by Kolesov et al. after a series of tests they performed on short-chain branched polyethylene; however, the occurrence of maximum recoverable work as a function of normalized recovered strain was not examined, nor was the effect of different temperatures taken into account.[31]

Figure 7(b) represents SMP work performed as a function of σ_A, for samples programmed at 20°C. For the samples programmed at 20°C, W_R behaved identical to the W_R of samples programmed at 70°C because at higher temperatures the recovered strain had a similar response independent of the programming temperature (Figs. 4 and 5). The overall trend of W_R as a function of σ_A was the same as before. It increased from zero, reached a maximum, and decreased until it reached zero again, similar to W_R. The W_{RMA} as a function of σ_A; however, yielded significantly different, asymmetric curves. For the same crosslinking density, the samples showed a sudden peak in W_{RMA} values for high σ_A values as shown with open circles. This significant increase in W_{RMA} values was attributed to the strain recovery peak that was observed for samples programmed at 20°C under higher values of σ_A (Fig. 5). This sudden increase in W_{RMA} was observed for all samples under high σ_A, independent of the crosslinking density. The magnitude of W_{RMA} also increased with the increase in the crosslinking density. This W_{RMA} peak has an important design implication, which suggests that in order to extract maximum work from the SMP under high constraining stress, they should be programmed
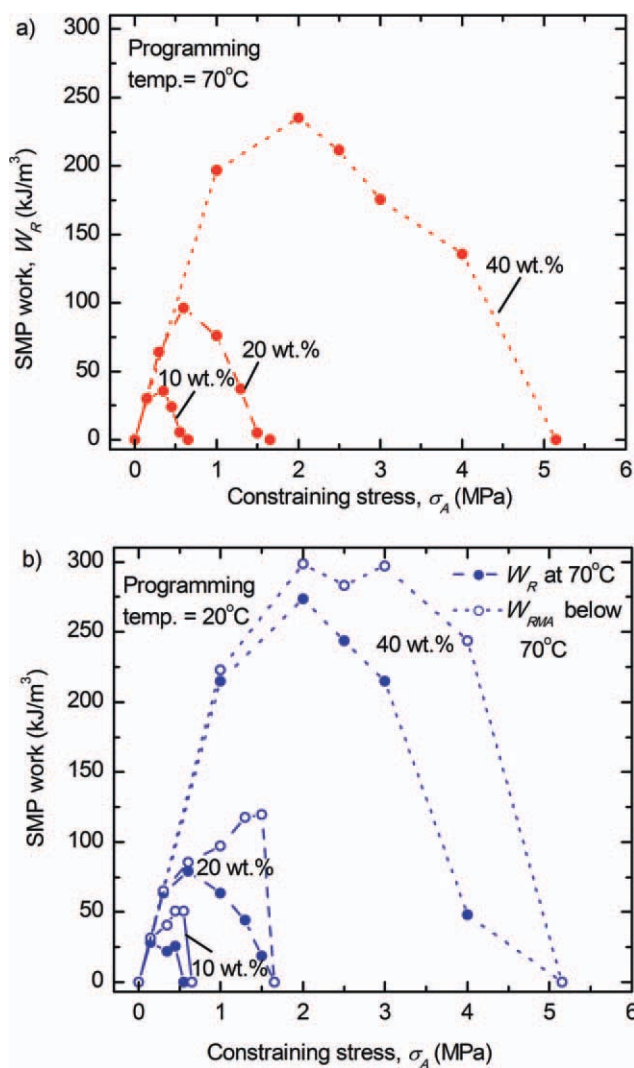
Figure 7 (a) SMP work performed as a function of constraining stress for a programming temperature of 70°C. Work performed was seen to be a symmetric, half-elliptical shape, as a function of constraining, exhibiting a maximum at ∼ 50% recovered strain. Work performed scaled with the crosslinking density, and (b) SMP work performed as a function of constraining stress for programming temperature of 20°C. The samples programmed at 20°C yielded higher maximum SMP work values for the same constraining stress. A significant peak in maximum SMP work (shown with open circles) was observed for higher constraining stress values, owing to the peak observed during strain recovery for samples programmed at 20°C. [Color figure can be viewed in the online issue, which is available at wileyonlinelibrary.com].

at temperatures below the T_g. However, under low constraining stresses, programming above or below the T_g, does not significantly change the maximum work performed by the SMP.

The maximum work efficiency of the SMP was also calculated. To accomplish this, it was required to first calculate the work necessary to deform the SMP by 30%, not including the stress relaxation. The energy required to initially deform the SMP was defined as the area underneath the stress–strain curve during initial compression. The work per unit volume required to deform the SMP, U, was calculated by numerically integrating the area under the stress–strain curve using Trapezoidal rule. Efficiency was therefore defined as the ratio of the maximum work performed by the SMP during recovery heating, relative to the work required to initially deform the SMP during the programming stage. Therefore, the efficiency is given by:

$$\eta = \frac{W_{\text{RMA}}}{U} \tag{4}$$

It was also important to consider the energy required for the initial deformation. The materials tested at 20°C will require more energy to be deformed to 30% strain owing to the reduced chain mobility of material being in the hard glassy state. Figure 8 shows η as a function of σ_A, for all samples tested. The efficiency followed a similar trend like the work performed by the SMP. It increased from zero for the unconstrained condition, reached a maximum and started to decrease again until it reached zero for the fully constrained condition. This trend was observed for all samples, independent of the crosslinking density and programming temperature.
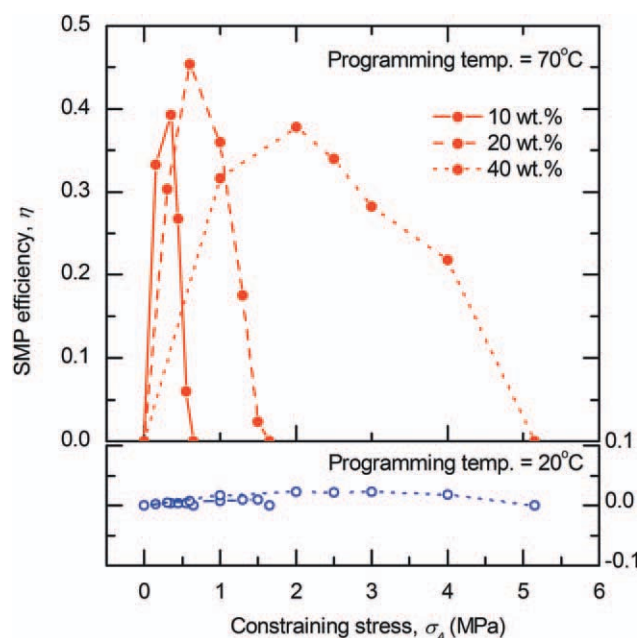
Figure 8 Efficiency of the SMP as a function of constraining stress. Efficiency is seen to be independent of the crosslinking densities of the SMPs. Maximum efficiency of the shape-memory effect is achieved in a partially constrained environment. Significant values of efficiency were obtained for programming temperature of 70°C, while the ones programmed at 20°C showed very low-efficiency values. [Color figure can be viewed in the online issue, which is available at wileyonlinelibrary.com.].

The curves were symmetric, half-elliptical with the maximum occurring in the proximity of 50% recovered strain. For the samples programmed at 70°C, the efficiency values and the overall trend were similar for all crosslinking densities. This was also true for all the samples programmed at 20°C. Samples programmed at 70°C were observed to give higher efficiency values for a particular σ_A as compared to the corresponding values for the samples programmed at 20°C. For example, at $\sigma_A = 1$ MPa, a 20 wt % XLS sample had an efficiency of about 36% when initially programmed at 70°C, and an efficiency of about 1% when initially programmed at 20°C. This was clearly because of the large stresses required to deform the samples in the glassy regime. Overall the efficiency values were very low for the samples programmed at 20°C, while the samples programmed at 70°C gave significant efficiency values from 28 to 45%. Figure 8 clearly showed that SMPs should be programmed at a higher temperature, in the rubbery region, to extract maximum efficiency from the networks.

CONCLUSIONS

Monotonic compressive testing was performed on meth(acrylate) based networks of different crosslinking densities with same glass transition temperature (T_g) and different rubbery modulus (E_r'). Samples were compressed at temperatures, above and below the T_g of the materials. Partially constrained recovery characterization was experimentally achieved by applying a constraining stress on the SMP while reheating it for strain recovery. Work performed by the SMP and its efficiency was calculated. Consequently, the following conclusions were derived:

1. An unreported strain recovery peak was observed under partially constrained conditions for samples programmed at temperature below T_g (20°C) and higher constraining stresses. A detailed parameter study is underway to investigate the underlying mechanisms of this strain recovery peak based on a thermo-viscoelastic model for amorphous SMP.
2. There was a near linear relationship between the strain recovered and the constraining stress applied to the SMP while heating it for recovery. This relationship holds true for samples deformed above or below T_g. Polymer networks with lower crosslinking densities will require lower constraining stresses, to match the same recovery strains as higher cross-linked networks.
3. The final value of the recovered strain for a given constraining stress correlates with the rubbery modulus (from DMA analysis), for any given temperature, which proves that the shape

recovery is driven by the entropic rearrangements of the amorphous network above the T_g to its equilibrium configuration. This holds true irrespective of the programming temperature being above or below the T_g.
4. Work performed by the shape-memory effect scales with crosslinking density, and thereby rubbery modulus. The networks with highest rubbery modulus gives the highest work performed, with maximum values observed when normalized strain recovered was close to 50% for samples programmed at 70°C. For samples programmed at 20°C, maximum work performed increased significantly with the increase in the applied constraining stress, which was a reflection of the strain recovery peak.
5. Efficiency is independent of crosslinking density for SMPs deformed above and below T_g. To extract the maximum efficiency from the SMPs, they should be initially programmed at temperatures in the rubbery regime. Significant efficiency values obtained varied from 28 to 45% and the maximum efficiency was achieved when 50% of the normalized-strain was recovered for all crosslinking densities. The samples initially programmed at temperatures in the glassy region demonstrate very low-efficiencies for all recovered strains, on the order of 1–3%.

References

1. Lendlein, A.; Behl, M. Soft Matter 2007, 3, 58.
2. Frick, C. P.; Ortega, A. M.; Tyber, J.; Maksound, A. E. M.; Maier, H. J.; Liu, Y. N.; Gall, K. Mater Sci Eng A Struct Mater Proper Microstruct Process 2005, 405, 34.
3. Shaw, J. A.; Kyriakides, S. J Mech Phys Solids 1995, 43, 1243.
4. Rousseau, I. A. Polym Eng Sci 2008, 48, 2075.
5. Voit, W.; Ware, T.; Dasari, R. R.; Smith, P.; Danz, L.; Simon, D.; Barlow, S.; Marder, S. R.; Gall, K. Adv Funct Mater 2010, 20, 162.
6. Luo, X. F.; Mather, P. T. Soft Matter 2010, 6, 2146.
7. Mather, P. T.; Luo, X. F.; Rousseau, I. A. Ann Rev Mater Res 2009, 39, 445.
8. Lendlein, A.; Langer, R. Science 2002, 296, 1673.
9. Yakacki, C. M.; Lyons, M. B.; Rech, B.; Gall, K.Shandas, R. Biomed Mater 2008, 3, 9
10. Yakacki, C. M.; Gall, K. Shape-Memory Polymers; Springer-Verlag Berlin: Berlin, 2010, p 147.
11. Dietsch, B; Tong, T. J Adv Mater Covina 2007, 39, 3.
12. Sokolowski, W. M.; Tan, S. C. J Spacecraft Rockets 2007, 44, 750.
13. Robin, J.; Martinot, S.; Curtil, A.; Vedrinne, C.; Tronc, F.; Franck, M.; Champsaur, G. J Thorac Cardiov Sur 1998, 115, 898.
14. Feninat, F. El.; Laroche, G.; Fiset, M.; Mantovani, D. Adv Eng Mater 2002, 4, 91.
15. Kane, R. S.; Takayama, S.; Ostuni, E.; Ingber, D. E.; Whitesides, G. M. Biomaterials 1999, 20, 2363.
16. Jackson, W. C.; Tran, H. D.; O'Brien, M. J.; Rabinovich, E.; Lopez, G. P. J Vac Sci Technol B 2001, 19, 596.
17. Gall, K.; Kreiner, P.; Turner, D.; Hulse, M. J Microelectromech Syst 2004, 13, 472.
18. Castro, F.; Westbrook, K. K.; Long, K. N.; Shandas, R.; Qi, H. J. Mech Time Depend Mat 2010, 14, 219.

19. Domeier, L.; Nissen, A.; Goods, S.; Whinnery, L.McElhanon, J. J Appl Polym Sci 2010, 115, 3217.
20. Behl, M.; Razzaq, M. Y.; Lendlein, A. Adv Mater 2010, 22, 3388.
21. Qi, H. J.; Nguyen, T. D.; Castro, F.; Yakacki, C. M.; Shandas, R. J Mech Phys Solids 2008, 56, 1730.
22. Nguyen, T. D.; Qi, H. J.; Castro, F.; Long, K. N. J Mech Phys Solids 2008, 56, 2792.
23. Gall, K.; Yakacki, C. M.; Liu, Y. P.; Shandas, R.; Willett, N.; Anseth, K. S. J Biomed Mater Res A 2005, 73A, 339.
24. Baer, G. M.; Small, W.; Wilson, T. S.; Benett, W. J.; Matthews, D. L.; Hartman, J.; Maitland, D. J. Biomed Eng Online 2007, 6, 8.
25. Wache, H. M.; Tartakowska, D. J.; Hentrich, A.; Wagner, M. H. J Mater Sci Mater Med 2003, 14, 109.
26. Yakacki, C. M.; Shandas, R.; Lanning, C.; Rech, B.; Eckstein, A.; Gall, K. Biomaterials 2007, 28, 2255.
27. Maitland, D. J.; Metzger, M. F.; Schumann, D.; Lee, A.; Wilson, T. S. Laser Surg Med 2002, 30, 1.
28. Yoo, H. J.; Jung, Y. C.; Sahoo, N. G.; Cho, J. W. J Macromol Sci B 2006, 45, 441.
29. Cho, J. W.; Kim, J. W.; Jung, Y. C.; Goo, N. S. Macromol Rapid Commun 2005, 26, 412.
30. Rapp, S.; Baier, H. Smart Mater Struct 2010, 19, 045018.
31. Kolesov, I. S.; Kratz, K.; Lendlein, A.; Radusch, H. J. Polymer 2009, 50, 5490.
32. Pandini, S.; Pegoretti, A.; Ricco, T. J Therm Anal Calorim 2008, 94, 825.
33. Nguyen, T. D.; Yakacki, C. M.; Brahmbhatt, P. D.; Chambers, M. L. Adv Mater 2010, 22, 3411.
34. Ortega, A. M.; Kasprzak, S. E.; Yakacki, C. M.; Diani, J.; Greenberg, A. R.; Gall, K. J Appl Polym Sci 2008, 110, 1559.
35. Yakacki, C. M.; Satarkar, N. S.; Gall, K.; Likos, R.; Hilt, J. Z. J Appl Polym Sci 2009, 112, 3166.
36. Yakacki, C. M.; Shandas, R.; Safranski, D.; Ortega, A. M.; Sassaman, K.; Gall, K. Adv Funct Mater 2008, 18, 2428.
37. Yakacki, C. M.; Willis, S.; Luders, C.; Gall, K. Adv Eng Mater 2008, 10, 112.
38. Liu, Y. P.; Gall, K.; Dunn, M. L.; McCluskey, P. Smart Mater Struct 2003, 12, 947.
39. Chen, X.; Nguyen, T. D. Mech Mater 2011, 43, 127.